# Towards Relative Altitude Estimation in Topological Navigation Tasks using the Global Appearance of Visual Information

Francisco Amorós, Luis Payá, Oscar Reinoso, David Valiente and Lorenzo Fernández
*Systems Engineering and Automation Department, Miguel Hernández University,*
*Avda. de la Universidad s/n, 03202, Elche, Alicante, Spain*

Keywords: Global-appearance Descriptors, Topological Navigation, Altitude Estimation, Zooming, Camera Coordinate Reference System, Orthographic View, Unit Sphere Image.

Abstract: In this work, we present a collection of different techniques oriented to the altitude estimation in topological visual navigation tasks. All the methods use descriptors based on the global appearance of the scenes. The techniques are tested using our own experimental database, which is composed of a set of omnidirectional images captured in real lightning conditions including several locations and altitudes. We use different representations of the visual information, including the panoramic and orthographic views, and the projection of the omnidirectional image into the uni sphere. The experimental results demonstrate the effectiveness of some of the techniques.

SCITEPRESS SCIENCE AND TECHNOLOGY PUBLICATIONS

## 1 INTRODUCTION

The richness of the information that visual systems provide and the multiple possibilities of configurations and applications make them a popular sensing mechanism in robotic navigation tasks. Among all the of visual sensors, we focus our work in omnidirectional vision. In the literature, we can find numerous examples where omnidirectional visual systems are employed in navigation tasks, such as (Winters et al., 2000).

Classical research into mobile robots equipped with vision systems have focused on local features descriptors, extracting natural or artificial landmarks from the image. With this information, it is possible to obtain image descriptors useful in navigation tasks. As an example, (Lowe, 1999) proposes SIFT, and (Bay et al., 2006) presents SURF.

On the other hand, global appearance approaches propose processing the image as a whole, without local feature extraction. These techniques have demonstrated a good accuracy on the floor plane navigation in both location and orientation estimation. (Chang et al., 2010) and (Payá et al., 2010) include some examples.

Nowadays, Unmanned Aerial Vehicles (UAVs) are becoming very popular as a platform in the field of robotic navigation research. In this sense, we can find in (Mondragón et al., 2010), (Han et al., 2012) and (Wang et al., 2012) different approaches that study the motion and attitude of UAVs using visual systems. Specifically, these works are based on image feature extraction or image segmentation in order to extract valuable information of scenes to create and improve navigation systems.

The aim of this paper is to extend the use of the global appearance descriptors to navigation applications where the altitude of the mobile robot changes. For that purpose, we suppose that the UAV is stabilized and the visual sensor has the same attitude, which corresponds with the perpendicular regarding the floor plane. In particular, we study the ability of altitude estimation using global appearance descriptors.

The algorithms presented in this work are tested using our own experimental database, composed of omnidirectional images acquired with a catadioptric vision system composed of an hyperbolic mirror and a camera.

From the omnidirectional scenes, we represent the visual information using different projections. Specifically, the panoramic and orthographic views, and the projection over the unit sphere (Roebert et al., 2008). The descriptors used and the altitude estimation techniques depends on the type of scene projection.

The remainder of the paper is structured as follows: Section 2 includes the global appearance descriptors we use in order to compress the visual in-


Amorós F., Payá L., Reinoso O., Valiente D. and Fernández L..
Towards Relative Altitude Estimation in Topological Navigation Tasks using the Global Appearance of Visual Information.
DOI: 10.5220/0004746301940201
In *Proceedings of the 9th International Conference on Computer Vision Theory and Applications* (VISAPP-2014), pages 194-201
ISBN: 978-989-758-003-1
Copyright © 2014 SCITEPRESS (Science and Technology Publications, Lda.)

formation. Section 3 discusses the different methods used with the purpose of finding the relative altitude between images acquired in a same point in the floor plane. In the next section, the database used in the experiments is presented. Section 5 gathers the experimental results, and finally, the main conclusions are included in section 6.

## 2 GLOBAL APPEARANCE DESCRIPTORS

In this section we include some techniques to extract the most relevant information from images to build a descriptor. In particular, we present descriptors based on the global appearance of scenes. These descriptors are computed working with the image as a whole, avoiding segmentation or landmarks extraction, trying to keep the amount of memory to a minimum.

Specifically, the three descriptors included are based on the representation of the visual information in the frequency domain using the Fourier Transform.

### 2.1 Fourier Signature

The Fourier Signature is defined in (Menegatti et al., 2004). This work demonstrates that it is possible to represent an image using the Discrete Fourier Transform of each row. So, we can expand each row of an image $\{a_n\} = \{a_0, a_1, \ldots, a_{N-1}\}$ into the sequence of complex numbers $\{A_n\} = \{A_0, A_1, \ldots, A_{N-1}\}$:

$$\{A_n\} = \mathcal{F}[\{a_n\}] = \sum_{n=0}^{N-1} a_n e^{-j\frac{2\pi}{N}kn}, \quad k = 0, \ldots, N-1. \tag{1}$$

Taking profit of the Fourier Transform properties, we just keep the first coefficients to represent each row since the most relevant information concentrates in the low frequency components of the sequence. Moreover, when working with omnidirectional images, the modulus of the Fourier Transform of the image's rows is invariant against rotations in the perpendicular plane of the image.

### 2.2 2D Fourier Transform

When we have an image f(x,y) with Ny rows and Nx columns, the 2D discrete Fourier Transform is defined through:

$$\mathcal{F}[f(x,y)] = F(u,v) = \frac{1}{N_y} \sum_{x=0}^{N_x-1} \sum_{y=0}^{N_y-1} f(x,y) e^{-2\pi j\left(\frac{ux}{N_x}+\frac{vy}{N_y}\right)},$$
$$u = 0, \ldots, N_x-1, v = 0, \ldots, N_y-1. \tag{2}$$

The components of the transformed image are complex numbers so it can be split in two matrices, one with the modules (power spectrum) and other with the angles. The most relevant information in the Fourier domain concentrates in the low frequency components. Another interesting property when we work with panoramic images is the rotational invariance, which is reflected in the shift theorem:

$$\mathcal{F}[f(x-x_0, y-y_0)] = F(u,v) \cdot e^{-2\pi j\left(\frac{ux_0}{N_x}+\frac{vy_0}{N_y}\right)},$$
$$u = 0, \ldots, N_x-1, v = 0, \ldots, N_y-1. \tag{3}$$

According to this property, the power spectrum of the rotated image remains the same of the original image and only a change in the phase of the components of the transformed image is produced. The variation in the phase values depends on the shift on the x-axis ($x_0$) and the y-axis ($y_0$).

### 2.3 Spherical Fourier Transform

Omnidirectional images can be projected onto the unit sphere when the intrinsic parameters of the vision system are known. Being $\theta \in [0, \pi]$ the colatitude angle, and $\phi \in [0, 2\pi)$ the azimuth angle, the projection of the omnidirectional image in the 2D sphere can be expressed as $f(\theta, \phi)$. In (Driscoll and Healy, 1994), it is shown that the spherical harmonic functions $Y_{lm}$ form a complete orthonormal basis over the unit sphere. Any square integrable function defined on the sphere $f \in L^2(s^2)$ can be represented by its spherical harmonic expansion as:

$$f(\theta, \phi) = \sum_{l=0}^{\infty} \sum_{m=-l}^{l} \widehat{f}_{lm} Y_{lm}(\theta, \phi), \tag{4}$$

with $l \in \mathbb{N}$ and $m \in \mathbb{Z}$, $|m| \leq l$. $\widehat{f}_{lm} \in \mathbb{C}$ denotes the spherical harmonic coefficients, and $Y_{lm}$ the spherical harmonic function of degree $l$ and order $m$ defined by

$$Y_{lm}(\theta, \phi) = \sqrt{\frac{2l+1}{4\pi} \frac{(l-m)!}{(l+m)!}} P_l^m(\cos\theta) e^{im\theta}, \tag{5}$$

where $P_l^m(x)$ are the associated Legendre functions.

As with the Fourier Signature and 2D Fourier Transform, it is possible to obtain a rotationally invariant representation from the Spherical Fourier Transform. Considering $B$ the band limit of $f$, the coefficients of $e = (e_1, ..., e_B)$ are not affected by 3D rotations of the signal, where

$$e_l = \sqrt{\sum_{|m| \leq l} |\widehat{f}_{lm}|^2}. \tag{6}$$

SCITEPRESS SCIENCE AND TECHNOLOGY PUBLICATIONS

In (Makadia et al., 2004), (McEwen and Wiaux, 2011), (Schairer et al., 2009), (Huhle et al., 2010) and (Schairer et al., 2011) it is possible to find more information and examples of applications of the Spherical Fourier Transform in navigation tasks.

# 3 ALTITUDE ESTIMATION METHODS

This section details the different techniques used to obtain a measurement of the relative altitude of a set of images captured from the same point in the floor plane. We make use of functions included in the Matlab toolbox *OCamCalib* (Scaramuzza et al., 2006) to calibrate the camera and to obtain different views of the visual information from the omnidirectional image.

## 3.1 Central Cell Correlation of Panoramic Images

Many algorithms are based on the panoramic view of the omnidirectional image as a input information of the navigation system, e.g. (Briggs et al., 2004).

In a panoramic image, the most distinctive information is usually located in the central rows of the scene, specially in outdoor environments, where the lower angles usually correspond to the floor, and the higher angles to the sky. Moreover, if a change in the altitude of the robot is produced both upwards or downwards, this area is less likely to go out of the camera field of view.

Taking this into account, we propose to compare the central rows of two images to estimate its relative altitude. For that purpose, the algorithm computes the descriptor of a cell that includes the middle image rows, and repeat the process for different cells situated above and below the first one. In the Fig. 1 we can see an example of an image and different cells applied to the scene. The central cell is in bold, and we can also appreciate the additional cells above and below it.


Figure 1: Panoramic Image Cells used to find the relative altitude between two scenes.

When we have captured an image from the same (x,y) coordinate but with different altitude, we compute the descriptor of its central cell, and compare it with all the descriptors obtained from the cells of the first image (that acts as a reference image). The comparison is carried out by means of the Euclidean distance.

We match the central cell of the new image with all the cells of the reference image using the minimum descriptor distance as a criteria. The comparison with a lower image distance denotes a higher correlation, and the height ($d$) associated with the reference image cell selected denotes the relative altitude of both images, indicated in pixels.

## 3.2 FFT2D Vertical Phase Lag

As stated in Section 2.2, the 2D Fourier Transform let us to detect a change in the order of both rows and columns of a matrix. Specifically, as Eq. 3 indicates, a circular rotation of the rows or columns of the original information produces a change in the phase information of the Fourier Transform components, since the power spectrum remains without change.

When we work with panoramic images, a rotation of the scene produces a circular shift in the rows of the scene. For that reason, we are able to estimate the phase lag between two rotated images captured in the same position.

Our aim is to extend this property to vertical variations. However, we can not extrapolate the idea directly. Unlike a rotation around the perpendicular focal axis of the camera, a change in the robot altitude does not only produce the shift of the information included in the panoramic image, since the movement also supposes a change in the camera field of view. So, new information is introduced in the current image at the same time that some rows disappear in the lower or higher part of the panoramic image depending on the vertical movement direction. Therefore, it is not exactly a circular rotation of the image rows, reason why it introduces some changes in the Fourier transform coefficients.

Moreover, if a change in the orientation in the camera is produced at the same time that a variation in its altitude, the effects of both changes are introduced in the Fourier coefficients' phase, being difficult to discern whether the phase difference between the transforms of tho images has been produced because of the vertical or the rotation movement.

Since this work is focused in the altitude estimation, we suppose that the panoramic images have the same orientation.

In order to estimate the vertical lag between two

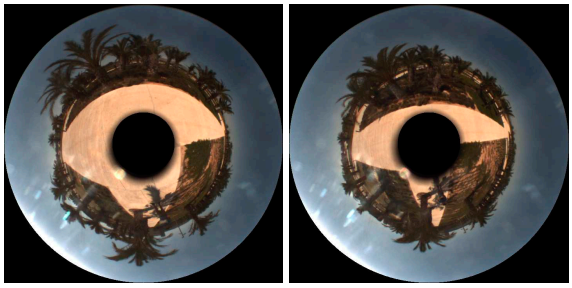

(a) Altitude=125cm($h = 1$) (b) Altitude=290cm($h = 12$)

Figure 2: Example of images captured at three different altitudes in the same location.

scenes captured from the same (x,y) location, we use the phase of the Fourier coefficients. Specifically, we use a submatrix with the first $N_F \times N_F$ elements of the 2D Transform phase, denoted by $ph(F_{N_F \times N_F})$.

As stated before, a vertical shift in the space domain produces a phase lag in the frequency space. We can artificially simulate the effect of a vertical rotation in the phase of the Fourier coefficients. Being $R$ the vertical rotation in degrees, the submatrix phase of the rotated coefficients $ph(F_{N_F \times N_F})_R$ can be estimated as:

$$ph(F_{N_F \times N_F})_R = ph(F_{N_F \times N_F}) + R \cdot VRM \qquad (7)$$

with $VRM$ the Vertical Rotation Matrix, that can be defined as:

$$VRM = \begin{pmatrix} 0 & 0 & \cdots & 0 \\ 1 & 1 & \cdots & 1 \\ 2 & 2 & \cdots & 2 \\ \vdots & \vdots & \ddots & \vdots \\ N_F & N_F & \cdots & N_F \end{pmatrix}_{N_F \times N_F} \qquad (8)$$

Given a reference image, we estimate $ph(F_{N_F \times N_F})_R$ for $R = [-180°, -180° + \Delta R, \ldots, 180°]$. In the experiments, we define $\Delta R = 0.5°$.

When an new image arrives, we compute $ph(F_{N_F \times N_F})$ and compare it with the different $ph(F_{N_F \times N_F})_R$ of the reference image.

The $R$ where the difference is minimum denotes the relative altitude between images.

### 3.3 Zooming of the Orthographic View

In this technique, we propose to make use of image zooming with the purpose of measuring the vertical shift of a UAV. In (Amorós et al., 2013), a method to obtain the topological distance between images following a route by means of zooming is developed.

However, we can not extract valuable information about altitude zooming the omnidirectional image directly. We need a representation of the visual information perpendicular to the movement movement. For that reason, we use the orthographic view of the scene. In (Maohai et al., 2013) and (Bonev et al., 2007) we can find examples where orthographic view is used in robot navigation tasks.

We vary the distance of the plane where the omnidirectional image is projected to obtain different zooms of the bird-eye view by changing the focal distance.

After obtaining the orthographic view, we need to describe the scene using two different descriptors. We can use both the Fourier Signature and the 2D Fourier Transform to describe the image.

We estimate the vertical distance between two images using the focal difference. First, we obtain the orthographic view of the reference image using several focal distances. The relative altitude of a new image captured in the same position in the floor plane, we project the bird-eye view of the new scene with a fixed focal, and compute its image distance with every projection of the reference view.

### 3.4 Coordinate Reference System (CRS) of the Camera

As shown in (Valiente et al., 2012), given an image, it is possible to modify the coordinate reference system (CRS) of the camera using the epipolar geometry, obtaining a new projection of the original image. The reprojected image, that uses the new CRS, reflects the movement of the camera.

Fist of all, we estimate the coordinates of the image in the real world in pixels. $m = [m_{x_{pix}}, m_{y_{pix}}]$ are the pixel coordinates regarding the omnidirectional image center. The camera calibration allows us to obtain the coordinates in the real world of the image. The image will be represented in the unit sphere $M \in \mathbb{R}^3$.

Then, we apply a change in the camera reference system:

$$M' = M + \rho \cdot T, \qquad (9)$$

being $T$ the unitary displacement vector in the z-axis, ($T = [0,0,1]^T$), and $\rho$ a scale factor proportional to the displacement of the CRS.

Once we have the new coordinates of the image $M'$, we can obtain the new pixel coordinates $m'$. Doing the association of the pixels of $m$ with the new coordinates $m'$, we obtain the new omnidirectional image that includes the camera CRS movement.

We have to take into account that when we match the correspondences between $m$ and $m'$, some pixel coordinates of the new image might lay outside the

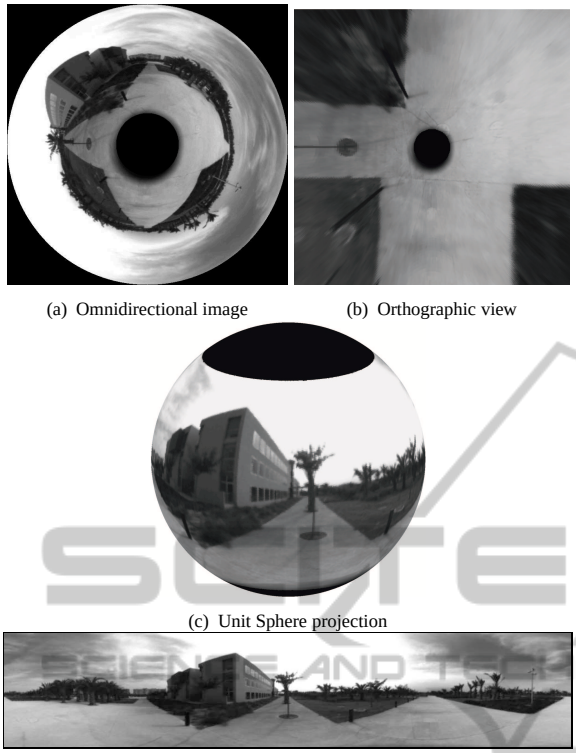

(a) Omnidirectional image (b) Orthographic view

(c) Unit Sphere projection

(d) Panoramic view

Figure 3: Different projections of the same image.

image frame, and some other pixels might not have associated any value. We interpolate the values of the pixels that do not have any association.

The altitude difference using this technique is represented by the displacement scale factor $\rho$.

After obtaining the new coordinates of the image, we need to gather the visual information using a descriptor. Note that from $M'$, we can obtain different representations of the visual information. Specifically, we use three different representations of the scene: the orthographic view of the omnidirectional image, the panoramic image, and the unit sphere. In Fig. 3, an example of each projection is shown.

We use the Fourier Signature and the 2D Fourier Transform to describe the orthographic and the panoramic views, whereas the Spherical Fourier Transform describes the unit sphere projection.

## 4 EXPERIMENTAL DATABASE

In order to carry out the experiments, we have acquired our own database of omnidirectional images in outdoor locations. We use a catadioptric system composed of a hyperbolic mirror and a camera with a resolution of 1280x960 pixels. The camera has been coupled to a tripod that allow us to have a range of 165cm in altitude.

The image acquisition has been done in 10 different locations. From every position, we capture 12 images in different altitudes. The minimum height is 125cm (h=1), and the maximum is 290cm (h=12), with a step of 15cm between consecutive images. In Fig. 2 we include some examples of database images varying $h$.

Therefore, the database is composed of 120 images captured in real lighting conditions. We do not vary the orientation of the images captured in a same location, although small rotations regarding the floor plane have been unavoidable.

In the database, we include images near and far from buildings, garden areas and a parking. We also vary the time when the images are captured to vary the illumination conditions and to have a more complete database.

In the experiments, we use different representations of the original visual information. Specifically, we compute the panoramic image, the orthographic view (or bird-eye view) and the projection onto the unit sphere. Fig. 3 includes an example of each representation.

## 5 EXPERIMENTS AND RESULTS

We test the altitude estimation methods included in Section 3 using two different experiments.

In the first experiment, we estimate the altitude of the images taking as a reference the scene in the lowest altitude ($h = 1$) for each location. The information that contains the database depends on the technique and global appearance descriptor used. The combination of the altitude estimation techniques with the different global appearance descriptors create 10 different possibilities.

In Fig.4 we include the mean value and standard deviation of the different altitude indicator tested in the different locations using $h = 1$ as a reference.

The second experiment is analogous to the first one, but we change the reference image. In this case, we choose the image corresponding to $h = 5$ (185 cm) as a reference, having test images both below and above the comparison image. Fig. 5 includes the mean value and standard deviation of the results for the 10 different locations.

Taking into account all the experimental results, we can confirm that the different methods present a monotonically increasing tendency as we increment the altitude lag between the compared images, with the exception of the Vertical 2D FFT Phase, and the

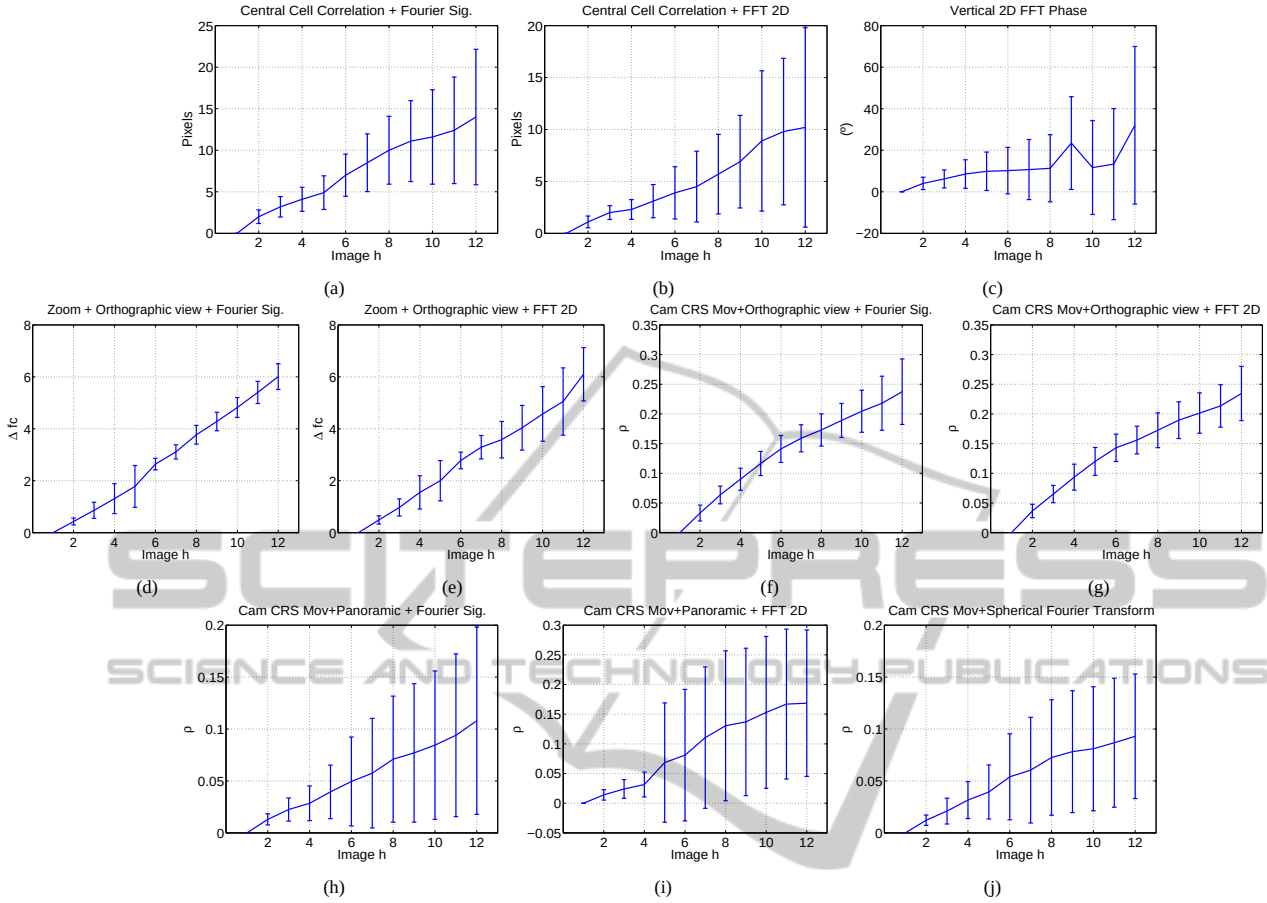


Figure 4: Experimental results estimating the altitude regarding the image with $h = 0$. Mean and standard deviation of all the different locations using the different methods.

Central Cell Correlation using FFT 2D for vertical lags greater than $h = 8$ (230 cm).

As a rule, the standard deviation increases as the test image distances from the reference, showing that the descriptors are less reliable. The experiments that use the orthographic view (independently of whether they use zooming or camera CRS movement), present a better accuracy in higher distances. On the other hand, the techniques using the panoramic view show the worst accuracy.

Considering the results of the second experiment included in Fig. 5, when the test images are below the reference, all the altitude indicators have negative sign. This allow us to determine the direction of the vertical movement. However, the Vertical 2D FFT Phase might present negative values despite having positive vertical displacements (Fig. 4(c)).

When we simulate the CRS movement described in Eq.(9), we are applying the same displacement in all the pixels of the image, independently of the distance of the object depicted in the scene. However, when we change the altitude of the camera in the real world, the objects included vary their position in the image depending on their relative position with the vision system. As an instance, the projection of objects that are far away from the camera suffers less changes than the projection of closer objects when we vary the sensor location.

This is particularly notable when we work with the panoramic view or the unit sphere projection, as we use almost the whole image, that usually includes information of objects placed in different distances from the camera system. On the contrary, the orthographic view usually include elements that are at a similar distance (near the floor plane). Despite this fact, the performance of all the algorithms that use the CRS camera displacement are acceptable until a altitude lag of 45cm ($\Delta h = 3$), although the orthographic view outperforms the panoramic and unit sphere projection.

Regarding the descriptor used to represent the image, the Fourier Signature presents better accuracy than Fourier 2D, being this difference specially remarkable in the Central Cell Correlation algorithm

SCITEPRESS SCIENCE AND TECHNOLOGY PUBLICATIONS

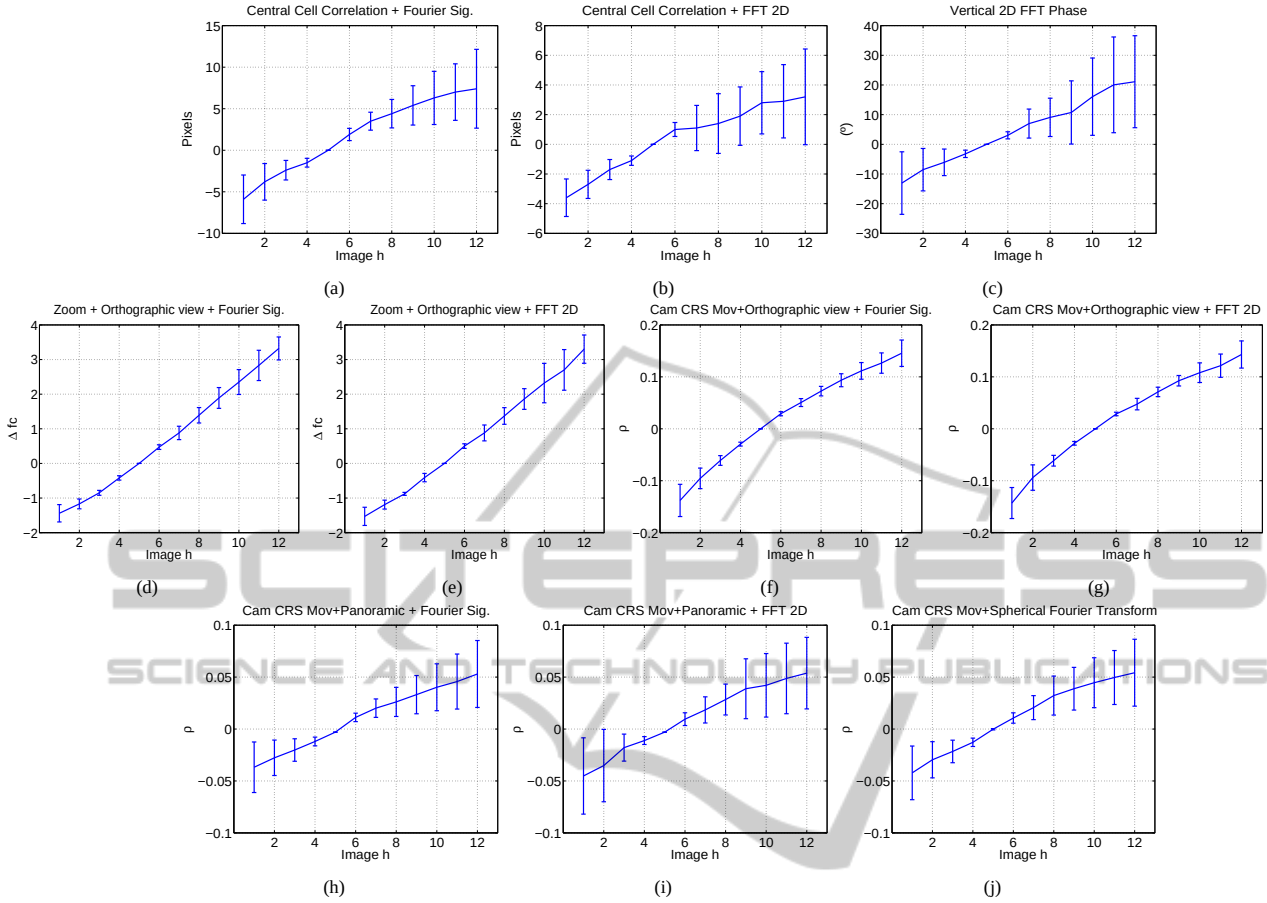


Figure 5: Experimental results estimating the altitude regarding the image with $h = 5$. Mean and standard deviation of all the different locations using the different methods.

(Fig. 4(a) and Fig. 4(b)).

In the experiments, we can also realize that the Spherical Fourier Transform over the unit sphere outperforms the Fourier Signature and the FFT 2D over the panoramic image. However, as stated above, the handicaps derived of the camera CRS movement technique affect the results.

All the experiments show that the Vertical Phase of the 2D Fourier Transform presents the lower accurate results. In the experimental database (Section 4), the images can present small rotations regarding the floor plane. These rotations affect directly the phase of the Transform coefficients (Eq. 3), and therefore, affects to the Vertical Phase estimation. The other techniques seem to deal better with these rotations.

## 6 CONCLUSIONS AND FUTURE WORK

In this work we have presented a comparison of different topological altitude estimation techniques applicable in UAVs navigation tasks using omnidirectional images. The approaches we included in this work describe the visual information using global appearance descriptors. The experiments have been carried out using our own database captured in a real environment under variable conditions.

The experimental results demonstrate that all methods proposed are able to estimate the relative altitude between two scenes captured in the same location for small altitude lags.

The techniques based on the orthographic view of the scene present a better accuracy, specially when we use the Camera CRS movement algorithm. However, the same technique over the panoramic view and the unit sphere projection presents not a reliable altitude indicator.

Regarding the descriptors used to compress the visual information, the Fourier Signature outperforms the 2D Fourier Transform. The Spherical Fourier Transform is the only descriptor that would let us to deal with 3D rotations in the space of the camera, al-

though combined with the camera CRS displacement technique does not allow to obtain a good accuracy for altitude lags greater than 185 cm.

All the methods deal with small rotations in the floor plane, except the Vertical 2D Fourier Transform Phase, since it is very sensitive to the change in the phase of the Fourier Transform coefficients.

The future work should extend this research to include topological distance estimation taking into account 6D movements and topological mapping.

## REFERENCES


Amorós, F., Payá, L., Reinoso, Ó., Mayol-Cuevas, W., and Calway, A. (2013). Topological map building and path estimation using global-appearance image descriptors. In *ICINCO 2013, International Conference on Informatics in Control, Automation and Robotics*.

Bay, H., Tuytelaars, T., and Gool, L. (2006). Surf: Speeded up robust features. In Leonardis, A., Bischof, H., and Pinz, A., editors, *Computer Vision at ECCV 2006*, volume 3951 of *Lecture Notes in Computer Science*, pages 404–417. Springer Berlin Heidelberg.

Bonev, B., Cazorla, M., and Escolano, F. (2007). Robot navigation behaviors based on omnidirectional vision and information theory. *Journal of Physical Agents*, 1(1):27–36.

Briggs, A. J., Detweiler, C., Mullen, P. C., and Scharstein, D. (2004). Scale-space features in 1d omnidirectional images. In *in Omnivis 2004, the Fifth Workshop on Omnidirectional Vision*, pages 115–126.

Chang, C.-K., Siagian, C., and Itti, L. (2010). Mobile robot vision navigation amp; localization using gist and saliency. In *Intelligent Robots and Systems (IROS), 2010 IEEE/RSJ International Conference on*, pages 4147–4154.

Driscoll, J. and Healy, D. (1994). Computing fourier transforms and convolutions on the 2-sphere. *Advances in Applied Mathematics*, 15(2):202 – 250.

Han, K., Aeschliman, C., Park, J., Kak, A., Kwon, H., and Pack, D. (2012). Uav vision: Feature based accurate ground target localization through propagated initializations and interframe homographies. In *Robotics and Automation (ICRA), 2012 IEEE International Conference on*, pages 944–950.

Huhle, B., Schairer, T., Schilling, A., and Strasser, W. (2010). Learning to localize with gaussian process regression on omnidirectional image data. In *Intelligent Robots and Systems (IROS), 2010 IEEE/RSJ International Conference on*, pages 5208–5213.

Lowe, D. (1999). Object recognition from local scale-invariant features. In *Computer Vision, 1999. The Proceedings of the Seventh IEEE International Conference on*, volume 2, pages 1150–1157 vol.2.

Makadia, A., Sorgi, L., and Daniilidis, K. (2004). Rotation estimation from spherical images. In *Pattern Recognition, 2004. ICPR 2004. Proceedings of the 17th International Conference on*, volume 3, pages 590–593 Vol.3.

Maohai, L., Han, W., Lining, S., and Zesu, C. (2013). Robust omnidirectional mobile robot topological navigation system using omnidirectional vision. *Engineering Applications of Artificial Intelligence*.

McEwen, J. and Wiaux, Y. (2011). A novel sampling theorem on the sphere. *Signal Processing, IEEE Transactions on*, 59(12):5876–5887.

Menegatti, E., Maeda, T., and Ishiguro, H. (2004). Image-based memory for robot navigation using properties of omnidirectional images. *Robotics and Autonomous Systems*, 47(4):251 – 267.

Mondragón, I. F., Olivares-Méndez, M., Campoy, P., Martínez, C., and Mejias, L. (2010). Unmanned aerial vehicles uavs attitude, height, motion estimation and control using visual systems. *Autonomous Robots, 29(1), 17-34*.

Payá, L., Fernández, L., Gil, A., and Reinoso, O. (2010). Map building and monte carlo localization using global appearance of omnidirectional images. *Sensors*, 10(12):11468–11497.

Roebert, S., Schmits, T., and Visser, A. (2008). Creating a bird-eye view map using an omnidirectional camera. In *BNAIC 2008: Proceedings of the twentieth Belgian-Dutch Conference on Artificial Intelligence*.

Scaramuzza, D., Martinelli, A., and Siegwart, R. (2006). A flexible technique for accurate omnidirectional camera calibration and structure from motion. In *Computer Vision Systems, 2006 ICVS '06. IEEE International Conference on*, page 45.

Schairer, T., Huhle, B., and Strasser, W. (2009). Increased accuracy orientation estimation from omnidirectional images using the spherical fourier transform. In *3DTV Conference: The True Vision - Capture, Transmission and Display of 3D Video, 2009*, pages 1–4.

Schairer, T., Huhle, B., Vorst, P., Schilling, A., and Strasser, W. (2011). Visual mapping with uncertainty for correspondence-free localization using gaussian process regression. In *Intelligent Robots and Systems (IROS), 2011 IEEE/RSJ International Conference on*, pages 4229–4235.

Valiente, D., Gil, A., Fernández, L., and Reinoso, Ó. (2012). View-based slam using omnidirectional images. In *ICINCO 2012 (2)*, pages 48–57.

Wang, C., Wang, T., Liang, J., Chen, Y., Zhang, Y., and Wang, C. (2012). Monocular visual slam for small uavs in gps-denied environments. In *Robotics and Biomimetics (ROBIO), 2012 IEEE International Conference on*, pages 896–901.

Winters, N., Gaspar, J., Lacey, G., and Santos-Victor, J. (2000). Omni-directional vision for robot navigation. In *Omnidirectional Vision, 2000. Proceedings. IEEE Workshop on*, pages 21–28.